

1

2 **Co-expression of *Foxa.a*, *Foxd* and *Fgf9/16/20* defines a transient mesendoderm**
3 **regulatory state in ascidian embryos**

4

5 **Clare Hudson^{§,*}, Cathy Sirour and Hitoyoshi Yasuo^{§,*}**

6 Sorbonne Universités, UPMC Univ Paris 06, CNRS, Laboratoire de Biologie du
7 Développement de Villefranche-sur-mer, Observatoire Océanologique, 06230, Villefranche-
8 sur-mer, France

9

10 §- These authors contributed equally to this work

11 *Correspondence:

12 email: hudson@obs-vlfr.fr or yasuo@obs-vlfr.fr

13 tel: +33 493763980

14 fax: +33 493763982

15

16 **Abstract**

17 In many bilaterian embryos nuclear β -catenin (n β -catenin) promotes mesendoderm over
18 ectoderm lineages. Although this is likely to represent an evolutionary ancient developmental
19 process, the regulatory architecture of n β -catenin-induced mesendoderm remains elusive in
20 the majority of animals. Here, we show that, in ascidian embryos, three n β -catenin
21 transcriptional targets, *Foxa.a*, *Foxd* and *Fgf9/16/20*, are each required for the correct
22 initiation of both the mesoderm and endoderm gene regulatory networks. Conversely, these
23 three factors are sufficient, in combination, to produce a mesendoderm ground state that can
24 be further programmed into mesoderm or endoderm lineages. Importantly, we show that the
25 combinatorial activity of these three factors is sufficient to reprogramme developing ectoderm
26 cells to mesendoderm. We conclude that in ascidian embryos the transient mesendoderm
27 regulatory state is defined by co-expression of *Foxa.a*, *Foxd* and *Fgf9/16/20*.

28

29 **Introduction**

30 The mesoderm, endoderm and ectoderm arise during embryonic development by a process
31 termed germ layer segregation. In many species, at least part of the endoderm and mesoderm
32 derive from transient ‘mesendoderm’ precursors, as is the case in ascidian embryos
33 (Kimelman and Griffin, 2000; Rodaway and Patient, 2001). However, the precise nature of
34 this induced regulatory state is not well understood. In ascidians, the first animal-vegetal (A-
35 V) oriented cell division generates the 8-cell stage embryo and segregates the mesendoderm
36 and some neural lineages into two pairs of vegetal founder lineages (the A- and B-line) and
37 the ectoderm (epidermis and neural) into two pairs of animal lineages (a- and b-line)
38 (Conklin, 1905; Nishida, 1987). This study focuses on the A-line mesendoderm lineages.
39 From the 8- to 16-cell stage, the two A4.1 blastomeres divide medio-laterally to generate the
40 two pairs of neuro-mesendodermal NNE cells, for notochord/neural/endoderm (Figure 1a).
41 NNE cells then divide along the A-V axis to generate NN cells (notochord/neural) and E
42 (mostly endoderm) cells at the 32-cell stage (Figure 1a). Subsequently, NN cells segregate
43 into notochord and neural lineages at the 64-cell stage. At this stage, while the medial E cell
44 generates two endoderm precursors, the lateral-most E cell is subject to an inductive
45 interaction resulting in the generation of one endoderm and one mesoderm (the trunk lateral
46 cell lineage) precursor (Shi and Levine, 2008). Later, during neural plate patterning, a muscle
47 precursor is also generated from the lateral borders of the NN-lineage derived neural plate
48 (Nicol and Meinertzhagen, 1988; Nishida, 1987). Thus, as in other species, ascidian germ
49 layer segregation can be viewed as a progressive process with part of the neural tissue arising
50 from bipotential neuro-mesodermal progenitors (Henrique et al., 2015; Tzouanacou et al.,
51 2009). The earliest cell divisions of the ascidian embryo along the A-V axis at the 8 and 32-
52 cell stages can be considered as the earliest steps of germ layer segregation.

53 β -catenin is a transcriptional co-activator which acts in a complex with TCF DNA-
54 binding proteins to mediate the canonical Wnt signalling pathway (Valenta et al., 2012). The
55 β -catenin/TCF complex promotes endoderm or mesendoderm in a wide range of organisms
56 and this process is therefore likely to represent an ancestral mechanism (Darras et al., 2011;
57 Henry et al., 2008; Hudson et al., 2013; Imai et al., 2000; Logan et al., 1999; McCauley et al.,
58 2015; Miyawaki et al., 2003; Momose and Houlston, 2007; Wikramanayake et al., 1998;
59 Wikramanayake et al., 2003). We have previously shown that the earliest steps of germ layer
60 segregation in ascidian embryos is mediated by two rounds of nuclear(n)- β -catenin-
61 dependent binary fate decisions. The first n β -catenin-driven binary fate decision takes place at
62 the 8-16-cell stage. During this process, the β -catenin/TCF complex is differentially activated
63 between mesendoderm and ectoderm progenitors, resulting in segregation of these lineages
64 (Figure 1a) (Hudson et al., 2013; Oda-Ishii et al., 2016; Rothbächer et al., 2007). The second
65 step takes place at the 32-cell stage and controls the segregation of NNE mesendoderm cells
66 into endoderm (E cell) and notochord/neural (NN cell) lineages (Hudson et al., 2013). During
67 this step the β -catenin/TCF complex is again differentially activated between E and NN cells
68 (Figure 1a). Therefore, cells in which n β -catenin remains active during the two steps (ON +
69 ON) are specified as endoderm lineage, cells in which n β -catenin remains inactive during the
70 two steps (OFF + OFF) are specified as ectoderm lineage and cells in which n β -catenin is
71 active during the first step but inactive during the second step (ON + OFF) are specified as
72 notochord-neural lineage (Hudson et al., 2013). These two rounds of n β -catenin-driven
73 switches result in transcriptional activation of the lineage specifiers, *Zic-related.b* (*Zic-r.b*,
74 formally *ZicL*) and *Lhx3/4* (formally *Lhx3*), in NN and E cells, respectively (Imai et al.,
75 2002b; Satou et al., 2001). One of the key features of these reiterative n β -catenin-driven
76 binary fate decisions is that the same asymmetric cue (n β -catenin) is interpreted differently
77 during each step (Bertrand and Hobert, 2010). Thus in the NNE lineage, it is likely that the

78 transient regulatory state induced by the first n β -catenin input in NNE cells confers a distinct
79 transcriptional response to the second n β -catenin input on E cells.

80 In this study, we characterise the NNE lineage specification factors, which are induced
81 by the first n β -catenin input, and address how these mesendoderm factors feed into the gene
82 regulatory network of the NN and E lineages.

83

84 Results

85 ***Foxa.a, Foxd and Fgf9/16/20 are n β -catenin transcriptional targets in NNE cells***

86 Following the first n β -catenin activation at the 16-cell stage, *Foxa.a*, *Foxd*, *Fgf9/16/20*,
87 *cadherinII* and *β CD1* (β -catenin downstream gene 1) are induced in the NNE cells, with at
88 least *Foxd* and *Fgf9/16/20* being direct targets of the β -catenin/Tcf7 complex (Imai, 2003;
89 Imai et al., 2002a; Imai et al., 2002b; Imai et al., 2002c; Kumano et al., 2006; Oda-Ishii et al.,
90 2016; Rothbächer et al., 2007; Satou et al., 2001). Consistent with a recent study (Oda-Ishii et
91 al., 2016), we confirmed that in β -catenin-inhibited (β -catenin-MO injected) embryos
92 analysed at the 16-cell stage, *Foxd* and *Fgf9/16/20* expression was lost (Figure 1b). In
93 addition to the mesendoderm lineages, *Foxa.a* is also expressed in the a-line anterior
94 ectoderm lineages in a n β -catenin-independent fashion (Figure 1b, c) (Lamy et al., 2006). In
95 β -catenin-inhibited embryos, *Foxa.a* expression persisted in NNE and a-lineage cells,
96 probably due to transformation of vegetal cells into animal cells that has been reported
97 previously (Figure 1b) (Imai et al., 2000; Oda-Ishii et al., 2016). Conversely, ectopic
98 stabilisation of n β -catenin resulted in activation of all three genes in ectoderm lineages at the
99 16-cell stage (Figure 1c). This was achieved by treating embryos with BIO, a chemical
100 inhibitor of the upstream inhibitory regulator of β -catenin, GSK-3, from the 8-cell stage

101 (Meijer et al., 2003). Thus, our results confirm that *Foxd*, *Foxa.a* and *Fgf9/16/20* are
102 transcriptional targets of n β -catenin in vegetal cells, though *Foxa.a* also has a n β -catenin-
103 independent expression in a-line animal cells.

104

105 ***Foxa.a, Foxd and Fgf9/16/20-signals are required for the correct initiation of both NN***
106 ***and E gene expression***

107 It is likely that these gene products, activated by the first n β -catenin signal in NNE cells, act
108 together with the second differential n β -catenin signal to activate the distinct gene regulatory
109 networks between NN and E cells. Consistent with this idea, *Foxa.a* has been shown to be
110 required for both NN lineage and endoderm gene expression (Imai et al., 2006), with *Foxd*
111 specifically required for NN lineage, but not endoderm fates, and *Fgf9/16/20* contributing to
112 notochord induction from the NN lineage (Imai et al., 2002a, 9; Imai et al., 2002c; Yasuo and
113 Hudson, 2007). However, we found that inhibiting any one of these factors prevented the
114 correct initiation of gene expression in both NN (*Zic-r.b*) and E (*Lhx3/4*) lineages (Figure 2a,
115 Table 1). We inhibited these factors using Morpholino anti-sense oligonucleotides (Foxyd-MO,
116 Foxa.a-MO, Fgf9-MO) and analysed *Zic-r.b* and *Lhx3/4* expression at the 32-cell stage, when
117 NN and E cell lineages become segregated. FGF signals are frequently mediated by the
118 MEK/ERK signalling pathway, leading to transcriptional activation via ETS family
119 transcription factors, as is the case in ascidian embryos (Bertrand et al., 2003; Kim and
120 Nishida, 2001; Miya and Nishida, 2003; Yasuo and Hudson, 2007). We confirmed that
121 *Fgf9/16/20* is responsible for the broad activation of ERK at the 32-cell stage in most vegetal
122 lineages, including NN and E lineages, as well as two neural lineages in the ectoderm (Figure
123 2-figure supplement 1f). Treatment of embryos from the 16-cell stage with the MEK inhibitor
124 U0126, also inhibits this ERK1/2 activation (Kim and Nishida, 2001; Picco et al., 2007).

125 Inhibition of Fgf9/16/20, MEK or ETS1/2 (ETS1/2-MO) gave similar results, although
126 inhibition of ETS1/2 gave only a weak down-regulation of *Zic-r.b* expression at the 32-cell
127 stage, perhaps indicating the involvement of additional transcription factors that are also
128 known to mediate FGF signals in *Ciona* embryos (Figure 2a; Table 1) (Bertrand et al., 2003;
129 Gainous et al., 2015). Maintenance of *Foxa.a*, *Foxd* and *Fgf9/16/20* expression at the 32-cell
130 stage are independent of each other (Figure 2-figure supplement 1a), as was shown previously
131 for *Foxd* and *Fgf9/16/20* in *Ciona savigni* embryos (Imai et al., 2002a).

132 In FGF-inhibited embryos, *Zic-r.b* expression recovered at the 64-cell stage (Figure 2-
133 figure supplement 1a) (Imai et al., 2006; Kumano et al., 2006). *Zic-r.b* expression at the 32-
134 and 64-cell stages can be mediated by separate enhancer elements (Anno et al., 2006). In
135 addition, in the NN-cell lineage, FGF-signalling is required for notochord fate, but has to be
136 attenuated for neural fate (Picco et al., 2007). Thus, an FGF-independent expression of *Zic-r.b*
137 at the 64-cell stage, at least in neural fated cells, is not unexpected. At the 64-cell stage,
138 FGF9/16/20 signals act again, to specify notochord over neural fates (Minokawa et al., 2001;
139 Yasuo and Hudson, 2007). Thus, there is an on-going requirement for FGF-signals during
140 notochord (mesoderm) specification. In *Foxa.a*- and *Foxd*- inhibited embryos, *Zic-r.b*
141 continues to be repressed in the NN-cell lineages at the 64-cell stage (Figure 2-figure
142 supplement 1a) and later (Imai et al., 2006), consistent with a requirement for *Foxa.a* and
143 *Foxd* for both NN cell lineage-derived structures, the notochord and caudal CNS (Imai et al.,
144 2002c; Imai et al., 2006),

145 Endoderm gene expression was continuously reduced up to at least the early gastrula
146 stage, following inhibition of any one of the NNE factors (Figure 2-figure supplement 1a-c).
147 However, using alkaline phosphatase activity as an indicator of endoderm formation
148 (Whittaker, 1977), a complete loss of endoderm at larval stages was observed only in *Foxa.a*-
149 inhibited embryos, consistent with previous studies (Figure 2-figure supplement 2) (Imai et

150 al., 2002c; Imai et al., 2006). In *Foxd* and FGF-signal inhibited embryos, a large domain of
151 alkaline phosphatase activity could be detected, suggesting that endoderm fate recovers in
152 these embryos (Figure 2-figure supplement 2). Simultaneous repression of *Foxd* and FGF-
153 signalling, however, resulted in both a stronger repression of early endoderm gene expression
154 as well as an almost complete absence of alkaline phosphatase activity at larval stages (Figure
155 2-figure supplement 1-2). Thus, for eventual endoderm formation, the embryo is able to
156 compensate for loss of either *Foxd* or FGF-signals, but is not able to compensate for loss of
157 both.

158 As well as promoting vegetal ‘mesendoderm’ fates, n β -catenin also represses the
159 ectoderm gene programme in vegetal cells (Hudson et al., 2013; Imai et al., 2000; Oda-Ishii et
160 al., 2016; Rothbächer et al., 2007). In β -catenin knock-down embryos, ectopic expression of
161 the early ectoderm gene *Efna.d* (formally *ephrin-Ad*) is observed in both NN and E cells at the
162 32-cell stage (Figure 2b) (Hudson et al., 2013) as well as in NNE cells at the 16-cell stage
163 (Oda-Ishii et al., 2016). Double inhibition of *Foxd* and FGF-signals also resulted in ectopic
164 expression of *Efna.d* in NN cells, but never in E cells (Figure 2b). Thus, NNE factors repress
165 the ectoderm genetic programme in NN cells. A lack of derepression in E cells is probably
166 due to the presence of n β -catenin in E cells at the 32-cell stage (Hudson et al., 2013),
167 suggesting that n β -catenin can repress the ectoderm genetic programme both via and
168 independently of the NNE factors.

169

170 **Combinatorial activity of Foxa.a, Foxd and Fgf9/16/20 induces a mesendoderm state**

171 Our data so far show that Foxa.a, Foxd and Fgf9/16/20-ERK1/2 are individually required for
172 the correct initiation of the genetic programmes of both NN and E cell lineages. Indeed, co-
173 expression of these three factors takes place only in mesendoderm lineages, the NNE and B-

line mesendoderm lineages of the 16- and 32-cell stage embryo (Figure 1; Figure 2-figure supplement 1a). At the 32-cell stage, the E cells continue to express these three genes, while NN cells express only *Foxa.a* and *Fgf9/16/20*. However, we have previously shown that *Foxd* transcripts preferentially segregate into the NN cells during the NN-E cell division, before they rapidly disappear (Hudson et al., 2013). Thus, NN cells also contain *Foxd* transcripts early in their cell cycle. We conclude that *Foxa.a*, *Foxd* and *Fgf9/16/20* are co-expressed only in mesendoderm lineages. We next addressed whether these three factors were sufficient to induce a mesendoderm regulatory state.

As well as in vegetal cells, *Foxa.a* is also expressed in a-line anterior animal cells and ERK1/2 is activated in one pair of a-line cells (the a6.5 pair) at the 32-cell stage (Figure 3a) (Hudson et al., 2003; Lamy et al., 2006). Thus, a6.5 cells possess two of the three mesendoderm lineage specifiers and yet they do not adopt an NNE-like lineage. Consistent with the notion that coexpression of *Foxa.a*, *Foxd* and *Fgf9/16/20* represents a NNE regulatory state, reintroduction of the remaining factor, *Foxd*, by mRNA injection, was able to convert a-line cells to a mesendoderm state (Figure 3). Injection of *Foxd* mRNA resulted in ectopic expression of *Zic-r.b* in a-line cells at the 32-cell stage (Figure 3b) (Imai et al., 2002b). Similarly, expression of *Bra*, a marker of notochord precursors, was induced at the 64-cell stage (Figure 3b). The broad ectopic expression of *Zic-r.b* and *Bra* in the a-lineage was clearly not restricted to the a6.5 cells. The most likely reason for this was that *Foxd* mRNA injection led to weak activation of *Fgf9/16/20* and strong inhibition of *Efna.d* expression in the ectoderm cells (Figure 3-figure supplement 1). *Efna.d* is a known antagonist of FGF-signals in *Ciona* and its inhibition results in widespread activation of ERK1/2 in ectoderm lineages (Ohta and Satou, 2013; Picco et al., 2007; Shi and Levine, 2008). Consistent with this, when *Foxd* mRNA-injected embryos were treated with U0126, the ectopic expression of *Zic-r.b* was reduced and *Bra* expression was completely suppressed,

199 mimicking the effect of MEK inhibition on endogenous *Zic-r.b* and *Bra* gene expression
200 (Figure 3b). Thus, injection of *Foxd* mRNA is sufficient to convert Foxa.a/ERK1/2-positive
201 a-line cells into mesoderm.

202 Injection of *Foxd* mRNA, however, was not sufficient to induce endoderm gene
203 expression in ectoderm cells (Figure 3c). This was expected since the two-step n β -catenin
204 binary fate decision model predicts that segregation of the endoderm lineage from the NNE
205 lineage requires a second round of n β -catenin activation (Figure 1a) (Hudson et al., 2013).
206 Accordingly, when *Foxd*-mRNA injected embryos were treated from the late 16-cell stage
207 with BIO in order to mimic the second input of n β -catenin activation, both *Zic-r.b* and *Bra*
208 were repressed and *Lhx3/4* ectopically activated in the a-line ectoderm cells (Figure 3b-c).
209 Thus, the NNE-like state induced in animal cells by *Foxd* mRNA injection behaves in the
210 same way as NNE state of unmanipulated embryos.

211 Taken together, these experiments provide strong evidence that the combinatorial
212 activity of Foxa.a, *Foxd* and *Fgf9/16/20*-ERK1/2 represents a NNE mesendoderm regulatory
213 state downstream of the first round of n β -catenin input. To further test this model, we
214 addressed whether co-expression of *Foxa.a*, *Foxd* and *Fgf9/16/20* was sufficient to rescue
215 mesoderm in β -catenin-knockdown embryos. β -catenin-MO injected embryos would express
216 only *Foxa.a* among the three genes (Figure 1b). We have shown that injection of *Foxd* mRNA
217 results in induction of low levels of *Fgf9/16/20* expression, together with a strong suppression
218 of *Efna.d* expression (Figure 3-figure supplement 1). Thus, injection of *Foxd* mRNA should
219 be sufficient to recapitulate a *Foxd/Foxa.a/Fgf9/16/20* overlap. Consistent with this, injection
220 of *Foxd* mRNA was able to rescue expression of NN-lineage genes (*Zic-r.b* and *Bra*) in n β -
221 catenin-MO embryos and, as expected, this recovery depended on an intact FGF-signalling
222 pathway (Figure 4). We conclude that co-expression of *Foxd+Foxa.a+Fgf9/16/20* is

223 sufficient to induce a mesendoderm regulatory state, which can then be further programmed
224 into mesoderm or endoderm lineage by manipulation of n β -catenin activity.

225

226 **Foxa.a, Foxd and Fgf9/16/20 act synergistically to reprogramme developing ectoderm**
227 **cells to a mesendoderm state**

228 We next addressed whether ectopic expression of *Foxd*, *Foxa.a*, and *Fgf9/16/20* was able to
229 reprogramme developing ectoderm to a mesendoderm state (Figure 5, Figure 5-figure
230 supplement 1). The upstream regulatory sequences of the *Fucosyltransferase-like* (FT) gene
231 becomes active in ectoderm cells from the 64-cell stage, when the ectoderm genetic
232 programme is already underway (Figure 5-figure supplement 1) and when these cells no
233 longer express *Foxa.a*, *Foxd* or *Fgf9/16/20* (Imai et al., 2004; Pasini et al., 2012). Using FT
234 promoter driven constructs (*pFT>Foxa.a*, *pFT>Foxyd* and *pFT>Fgf9/16/20*), we expressed
235 *Foxa.a*, *Foxd* and *Fgf9/16/20* in different combinations in ectoderm lineages. To simplify the
236 analysis and to rule out the possibility that signals from the vegetal cells may influence the
237 experimental outcome, animal hemispheres of electroporated embryos were isolated by
238 micro-dissection at the 8-cell stage. Isolated explants were cultured until the neurula stage
239 when they were assayed for *Bra* expression (Figure 5a-b). *Bra* was chosen for this assay for
240 its mesoderm (notochord)-specific expression. We observed a clear combinatorial effect
241 between *Foxa.a*, *Foxd* and *Fgf9/16/20* on the reprogramming of ectoderm to mesoderm, with
242 strong induction of *Bra* seen only when all three constructs were co-electroporated (Figure
243 5b). This reprogramming was accompanied by a strong downregulation of ectoderm gene
244 expression and ectopic expression of *Zic-r.b* in the ectoderm cells of whole embryos (Figure
245 5-figure supplement 1). Furthermore, ectoderm explants could be reprogrammed to adopt an
246 endoderm state (Figure 5c). To achieve this, ectoderm explants from embryos electroporated

247 with the triple combination (*pFT>Foxa.a*, *pFT>Foxyd* and *pFT>Fgf9/16/20*) were treated with
248 a pulse of BIO from the 76-cell stage to mimic the second round of n β -catenin activation that
249 normally drives the segregation of NN and E lineages (Figure 5c). The 76-cell stage was
250 chosen, as at this stage ectopic expression driven by the *pFT* constructs is readily detectable
251 (Figure 5-figure supplement 1 a), the ectoderm programme is downregulated (Figure 5-figure
252 supplement 1 b) and ectopic *Zic-r.b* is not yet detected (Figure 5-figure supplement 1 c). This
253 stage thus represented the best approximation of the NNE state of normal embryos. We
254 confirmed that BIO-treatment was able to induce nuclear translocation of β -catenin in isolated
255 explants at the 76-cell stage (Figure 5-figure supplement 2). Endoderm induction was assayed
256 by detection of *Lhx3/4* expression at the mid-gastrula stage, that is approximately one hour
257 after the onset of BIO-treatment. Coupling these three factors with BIO-treatment resulted in
258 strong induction of *Lhx3/4* expression. We conclude that the combinatorial activity of *Foxa.a*,
259 *Foxyd* and *Fgf9/16/20* is sufficient to reprogramme developing ectoderm cells to adopt a
260 mesendoderm state.

261

262 **Discussion**

263 In this study, we have identified *Foxa.a*, *Foxyd* and *Fgf9/16/20* as the mesendoderm lineage
264 specifiers of the NNE cell. Transcriptional activation of *Foxa.a*, *Foxyd* and *Fgf9/16/20* is
265 induced by the first n β -catenin switch (Figure 1a, 6a). Co-expression of these three factors is
266 sufficient to reprogramme ectoderm cells to adopt a mesendoderm state. This ectopic
267 mesendoderm state can be further converted into either mesoderm or endoderm by
268 modulating n β -catenin activation.

269

270 **A model for ascidian germ layer segregation**

271 We propose the following model to summarise the initial stages of germ layer segregation in
272 ascidian embryos (Figure 6a). At the 8-to 16-cell stage of development, n β -catenin, activated
273 specifically in vegetal cells by as yet unknown mechanisms, promotes *Foxa.a*, *Foxd* and
274 *Fgf9/16/20* expression and represses ectoderm gene expression (Hudson et al., 2013; Imai et
275 al., 2000; Oda-Ishii et al., 2016; Rothbächer et al., 2007). *Foxa.a*, *Foxd* and *Fgf9/16/20*, are
276 co-expressed exclusively in mesendoderm lineages at the 16-32 cell stage of development
277 (Imai et al., 2002a; Imai et al., 2002c; Oda-Ishii et al., 2016), where they are required,
278 individually, for the correct initiation of both NN and E cell lineage gene expression at the 32-
279 cell stage (Figure 2). The NNE factors are also required to repress ectoderm gene expression:
280 co-repression of *Foxd* and *Fgf9/16/20* resulted in ectopic ectoderm gene expression in NN
281 cells (Figure 3) and *Foxd* overexpression alone was able to repress ectoderm gene expression
282 (Figure 3-figure supplement 1). However, our data also suggests that n β -catenin can repress
283 ectoderm gene expression independently of these three factors (Figure 3). Recently, it has
284 been shown that this can take place via a physical interaction between β -catenin/Tcf7 and
285 Gata.a, preventing this key regulator of ectoderm lineage from binding to its DNA target sites
286 (Oda-Ishii et al., 2016; Rothbächer et al., 2007).

287 Following inhibition of *Foxa.a*, *Foxd* or *Fgf9/16/20*, both endoderm and mesoderm
288 development is perturbed at later stages of development, although there is a redundancy
289 between *Foxd* and FGF-signalling for the eventual recovery of endoderm (Figure 2 and
290 supplements) (Imai et al., 2002a; Imai et al., 2002b; Imai et al., 2002c; Imai et al., 2006;
291 Kumano et al., 2006). It is likely that these factors play on-going roles during mesoderm and
292 endoderm lineage progression. For example, ERK1/2 activity is detected in both notochord
293 and endoderm until the early gastrula stage (Nishida, 2003; Yasuo and Hudson, 2007),
294 *Fgf9/16/20* is required at the 64-cell stage for induction of notochord and repression of neural
295 gene expression in the notochord lineage (Imai et al., 2002a; Kim and Nishida, 2001;

296 Minokawa et al., 2001; Yasuo and Hudson, 2007) and *Foxa.a* is continuously expressed in
297 notochord and endoderm, suggesting an on-going role for *Foxa.a* in both of these lineages
298 (Imai et al., 2004).

299 Importantly, creating ectopic zones of co-expression of these three factors in distinct
300 embryological settings, revealed their strong synergistic ability to induce a mesendoderm
301 state, which can be further programmed to an NN or E lineage by modulation of n β -catenin
302 levels (Figures 3-5 and supplements). We conclude that *Foxa.a*, *Foxd* and *Fgf9/16/20* are
303 crucial for the mesendoderm ground state that canalises the daughter lineages to adopt either
304 E or NN fates depending on the status of the second n β -catenin input.

305 It is important to bear in mind that the germ layers are still not fully segregated at the
306 32-cell stage. While this manuscript has focused on the mesendoderm fates that arise from the
307 NNE lineage, this lineage also produces neural tissue. NNE cells divide into E cells and NN
308 cells. In addition to notochord, the NN cell generates the posterior part of the CNS, including
309 the equivalent of the ‘spinal cord’ of vertebrates (reviewed in (Hudson, 2016)). The binary
310 cell fate decision between neural and notochord takes place at the 64-cell stage (Minokawa et
311 al., 2001; Picco et al., 2007). The lateral neural progenitors that arise from the NN-cell lineage
312 also produce a muscle cell during neural plate patterning, following another neuromesodermal
313 binary fate decision (reviewed in (Hudson and Yasuo, 2008)). Bipotential neuromesoderm
314 progenitors are not an ascidian novelty (Henrique et al., 2015; Tzouanacou et al., 2009). For
315 example, in the zebrafish tailbud, bipotential neuromesodermal progenitor cells generate
316 notochord and floorplate (ventral spinal cord) (Row et al., 2016) and in both human and
317 mouse embryonic stem cells and zebrafish tailbud stem cells, bipotential neuromesodermal
318 progenitors generate paraxial mesoderm and posterior neural tube (Gouti et al., 2014; Martin
319 and Kimelman, 2012). Even in the classical mesendoderm model, that is the *C. elegans* EMS
320 cell, the MS (mesoderm) lineage also gives rise to some neurons (Sulston and Horvitz, 1977;

321 Sulston et al., 1983). The lateral E cells of *Ciona* are also not yet fate-restricted to endoderm
322 fate. At the 64-cell stage of development the lateral E cell divides into one endoderm and one
323 trunk lateral cell (mesenchyme) precursor, following induction of trunk lateral cell fate (Shi
324 and Levine, 2008). Thus, as in other species, ascidian germ layer segregation is an progressive
325 process (Tzouanacou et al., 2009) and NNE specification should thus be considered as its first
326 step.

327

328 **Regulatory architectures of mesendoderm**

329 We have shown that, in ascidian embryos, individual mesendoderm lineage specifiers are
330 required for the initiation of both mesoderm and endoderm GRNs (Figure 6). Furthermore, we
331 have shown that the combinatorial activity of just three NNE factors is sufficient to
332 reprogramme developing ectoderm cells to a mesendoderm state. The mesendoderm
333 regulatory state in ascidian embryos is similar to the situation in the *C. elegans* EMS cell in
334 which the MED1/2 GATA factors feed into both E (endoderm) and MS (mesoderm) lineage
335 specification, such that MED1/2 directly activates both MS and E target genes (Broitman-
336 Maduro et al., 2005; Maduro et al., 2001; Maduro et al., 2015; McGhee, 2013). Similarly,
337 Foxa.a and Foxd can bind to the upstream sequences of both *Zic-r.b* (NN lineage) and *Lhx3/4*
338 (E lineage), suggesting that this genetic interaction is direct (Kubo et al., 2010). While there is
339 little doubt that mesendoderm transiently forms during embryogenesis of many animal
340 models, and that both mesoderm and endoderm are induced by similar upstream regulators (β -
341 catenin in invertebrates, β -catenin and Nodal in vertebrates), in most cases the transcriptional
342 nature of the mesendoderm state does not appear to be similar to that of ascidians or
343 nematodes. In particular, the existence of mesendoderm lineage specifiers (that is individual
344 factors required for the initiation of both mesoderm and endoderm GRNs) have not been

described in the majority of model organisms. For example, in sea urchins and anamniote vertebrates, mesendoderm has been described as a mixed regulatory state with simultaneous activation of mesoderm and endoderm GRNs, prior to the lineage segregation of these fates (Peter and Davidson, 2010; Rodaway and Patient, 2001). This type of ‘mixed-lineage’ regulatory architecture is also described in other systems and displays characteristics of multi-lineage priming, whereby the GRNs of two lineages are simultaneously activated prior to lineage segregation (Figure 6c) (Graf and Enver, 2009; Nimmo et al., 2015). If this were the scenario for the ascidian mesendoderm regulatory state, one would expect individual NNE factors to be required for, and be able to induce, only one or other of the two subsequent lineages (NN or E), but not both. A ‘mixed-lineage’ regulatory architecture is therefore not consistent with our data describing the NNE mesendoderm regulatory state (Figure 6).

These two regulatory architectures are, however, unlikely to be mutually exclusive. In sea urchin and sea stars, for example, genes interacting with both mesoderm and endoderm GRNs have been identified (<http://sugp.caltech.edu/endomes/>) (Davidson et al., 2002; McCauley et al., 2015). It cannot be ruled out that mesendoderm lineage specifiers, acting upstream of both endoderm and mesoderm GRNs, are more broadly utilised, but are simply difficult to uncover due to the sheer complexity of early embryos and their GRNs (Ben-Tabou de-Leon and Davidson, 2009; Kiecker et al., 2016; Tremblay, 2010). It is also possible that the regulatory architecture of nematode and ascidian mesendoderm resulted from an adaption to a lineage-based mode of development with small numbers of cells, perhaps enabling these rapidly developing embryos to bypass the need for cross-repression and prolonged stabilisations of the endoderm and mesoderm GRNs. In summary, it is not yet clear whether an obligate mesendoderm state (that is a state with mesendoderm lineage specifiers) is present in the majority of metazoan developmental programmes, though this seems to be the case in nematode and ascidian embryos.

370

371 **Methods**

372 **Overexpression and knockdown tools**

373 Morpholinos (MOs) were purchased from GeneTools and have been reported previously: β -
374 catenin-MO (Hudson et al., 2013); Foxa.a-MO and Foxd-MO (Imai et al., 2006); Fgf9/16/20-
375 MO and Fgf8/17/18-MO (Yasuo and Hudson, 2007), ETS1/2-MO (Bertrand et al., 2003).

376 Foxa.a-MO was injected at 0.85mM and ETS1/2-MO at 0.75mM. All other morpholinos were
377 injected at 0.5mM. U0126 was used at 2 μ M and BIO (GSK-3 inhibitor IX) at 2.5 μ M (both
378 were purchased from Calbiochem). Since a full-length cDNA clone for *Ciona intestinalis*
379 *Foxd* is not available in gene collection plates (Gilchrist et al., 2015; Satou et al., 2002), we
380 synthesized the *Ciona savignyi Foxd* mRNA from pRN3-Cs-Foxd (Imai et al., 2002c) using
381 mMESSAGEmACHINE kit (Thermo Fisher Scientific). The *Ciona savignyi Foxd* used in
382 this study corresponds to Genbank accession number AB057738.1. *Foxd* mRNA was injected
383 at 75ng/ μ l. In order to generate pFT>Foxa.a, pFT>Foxy and pFT>Fgf9/16/20, we first
384 constructed Gateway (Invitrogen) pENTR clones containing ORFs of these genes. ORFs of
385 *Cs-Foxd*, *Foxa.a* and *Fgf9/16/20* were PCR-amplified using the following primer pairs and
386 templates:

387 Foxa.a-attB1 (aaaaagcaggctaccATGATGTTGTCGTCTCCACC) and Foxa.a-attB2
388 agaaagctgggtTTAGCTTGCTGGTACGCAC) on cicl044j20 template; FGF9-attB1
389 (aaaaagcaggctaccATGTCTATGTTAACCAACATGTTAGG) and FGF9-attB2
390 (agaaagctgggtTCAGTAGAGTCGCCAGACTAC) on citb007k01; CsFoxyd-attB1
391 (aaaaagcaggctaccATGACTGTGGACTCTTGTACAG) and CsFoxyd-attB2
392 (agaaagctgggtCTAAATAAGTTTACGGGAATGG) on pRN3-Cs-Foxd. The
393 *Fucosyltransferase-like* driver has been reported previously (Pasini et al., 2012). The

394 promoter region was PCR-amplified using the following pair of primers to generate a
395 destination vector pSP1.72BSSPE-pFT::RfA-venus (Roure et al., 2007): pFT-attB3
396 (ggggacaagttgtataataaaggtaggetGGCATCATAACGTACAACCTG) and pFT-attB5
397 (ggggaccacttgtataaaaagttgggtTGCAGCGGTAGAGTTACTATTATC). pFT>Foxa.a,
398 pFT>Foxd and pFT>Fgf9/16/20 were then generated by LR reaction between corresponding
399 pENTR clones and pSP1.72BSSPE-pFT::RfA-venus.

400

401 **Embryological experiments.**

402 Adult *Ciona intestinalis* were purchased from the Station Biologique de Roscoff (France).
403 Blastomere names, lineage and the fate maps are previously described (Conklin, 1905;
404 Nishida, 1987). Ascidian embryo culture and microinjection have been described (Sardet et
405 al., 2011). All microinjections were carried out in unfertilised eggs. The electroporation
406 protocol was based on (Christiaen et al., 2009). Up to 60 µg of circular plasmid DNA was
407 made up to 250 µl at 0.6M mannitol. DNA/mannitol solution was mixed with 100 µl of
408 eggs in artificial sea water supplemented with 0.5% BSA (to help prevent sticking).
409 Electroporation was carried out at 50V for 16ms using a BTX ECM 830 and electroporated
410 embryos transferred to agarose-coated dishes. For data shown in Figure 4-figure supplement
411 1a, 50 µg of pFT>Foxd was used. Otherwise, each FT construct was used at 20 µg to give a
412 maximum total of 60 µg. pFT>tdTomato was used as a control electroporation at 60 µg. In all
413 experiments, embryos that failed to develop were discarded and all other embryos scored. All
414 data were pooled from at least two independent experiments (i.e. on different batches of
415 embryos).

416 The experimental design of the BIO treatment of electroporated ectodermal explants,
417 shown in Figure 5c, is as follows. Embryos were electroporated with three plasmids,

418 pFT>Foxa.a + pFT>Foxd + pFT>Fgf9/16/20. Ectoderm explants were isolated at the 8-cell
419 stage from control (unelectroporated) and electroporated embryos. Each sample of explants
420 was split into two groups and one group of each treated with BIO from the 76-cell stage. BIO
421 treatment was continued until fixation, when sibling embryos reached the mid-gastrula stage.
422 Explants remained in BIO for approximately 1 hour at 20°C.

423

424 **In situ hybridisation, gene naming, alkaline phosphatase staining, dpERK and β-catenin**
425 **immunofluorescence**

426 All gene markers used for in situ hybridisation have previously been described (Hudson et al.,
427 2013; Imai et al., 2004) (<http://ghost.zool.kyoto-u.ac.jp>). According to recent nomenclature
428 guidelines, we used *Zic-r.b* (previously called *ZicL*) to describe the 5 copies of *ZicL* gene
429 named *Zic-r.b – Zic-r.f, Lhx3/4* (previously *Lhx3*) and *Efna.d* (previously *ephrin-Ad*) (Stolfi et
430 al., 2015). The in situ hybridisation and alkaline phosphatase staining protocols are previously
431 described (Hudson et al., 2013). All single embryo panels, except those in Figure 3c, were
432 mounted in 50-80% glycerol and photographed on an Olympus BX51 using a Leica
433 DFC310FX camera. All multi-embryo panels as well as single-embryo panels in Figure 3c
434 were taken of embryos in PBT on a Leica Macroscope Z16 APO with a Canon EOS 60D
435 camera. The dpERK and β-catenin immunofluorescence protocols are described previously
436 (Haupaix et al., 2014; Hudson et al., 2013). Immunostained embryos were mounted in
437 Vectorshield-DAPI (Vector laboratories), analysed on a Leica SP5 confocal microscope and
438 processed with Image J.

439

440 **Competing Interests**

441 The authors declare no competing interests.

442

443 **Author Contributions**

444 CH, Conception and design, Acquisition of data, Analysis and interpretation of data, Drafting
445 or revising the article, Contributed unpublished, essential data, or reagents. HY, Conception
446 and design, Acquisition of data, Analysis and interpretation of data, Drafting or revising the
447 article, Contributed unpublished, essential data, or reagents. CS, Acquisition of data, Analysis
448 and interpretation of the data.

449

450 **Acknowledgements**

451 We thank U. Röthbacher and P. Lemaire (FT promoter), H. Nishida (β -catenin antibody), Y.
452 Satou (pRN3-Cs-Foxd and Foxa.a-MO) and N. Satoh (Gene Collection Plates) for tools,
453 Evelyn Houliston and David McClay for critical reading of the manuscript and helpful
454 discussions and Jenifer Croce and David McClay for interesting discussions on sea urchin
455 mesendoderm GRNs.

456

457 **References**

- 458 **Anno, C., Satou, A. and Fujiwara, S.** (2006). Transcriptional regulation of ZicL in the
459 *Ciona intestinalis* embryo. *Dev. Genes Evol.* **216**, 597–605.
- 460 **Ben-Tabou de-Leon, S. and Davidson, E. H.** (2009). Experimentally based sea urchin
461 gene regulatory network and the causal explanation of developmental phenomenology.
462 *Wiley Interdiscip Rev Syst Biol Med* **1**, 237–246.
- 463 **Bertrand, V., Hudson, C., Caillol, D., Popovici, C. and Lemaire, P.** (2003). Neural tissue
464 in ascidian embryos is induced by FGF9/16/20, acting via a combination of maternal
465 GATA and Ets transcription factors. *Cell* **115**, 615–627.

- 466 **Broitman-Maduro, G., Maduro, M. F. and Rothman, J. H.** (2005). The noncanonical
467 binding site of the MED-1 GATA factor defines differentially regulated target genes in the
468 *C. elegans* mesendoderm. *Dev. Cell* **8**, 427–433.
- 469 **Christiaen, L., Wagner, E., Shi, W. and Levine, M.** (2009). Electroporation of transgenic
470 DNAs in the sea squirt *Ciona*. *Cold Spring Harb Protoc* **2009**, pdb.prot5345.
- 471 **Conklin, E. G.** (1905). The organisation and cell lineage of the ascidian egg. *J. Acad. Natl.
472 Sci. (Philadelphia)* 1–119.
- 473 **Darras, S., Gerhart, J., Terasaki, M., Kirschner, M. and Lowe, C. J.** (2011). β -catenin
474 specifies the endomesoderm and defines the posterior organizer of the hemichordate
475 *Saccoglossus kowalevskii*. *Development* **138**, 959–970.
- 476 **Davidson, E. H., Rast, J. P., Oliveri, P., Ransick, A., Calestani, C., Yuh, C.-H.,
477 Minokawa, T., Amore, G., Hinman, V., Arenas-Mena, C., et al.** (2002). A Genomic
478 Regulatory Network for Development. *Science* **295**, 1669–1678.
- 479 **Gainous, T. B., Wagner, E. and Levine, M.** (2015). Diverse ETS transcription factors
480 mediate FGF signaling in the *Ciona* anterior neural plate. *Dev. Biol.*
- 481 **Gilchrist, M. J., Sobral, D., Khoueiry, P., Daian, F., Laporte, B., Patrushev, I.,
482 Matsumoto, J., Dewar, K., Hastings, K. E. M., Satou, Y., et al.** (2015). A pipeline for the
483 systematic identification of non-redundant full-ORF cDNAs for polymorphic and
484 evolutionary divergent genomes: Application to the ascidian *Ciona intestinalis*. *Dev. Biol.*
485 **404**, 149–163.
- 486 **Gouti, M., Tsakiridis, A., Wymeersch, F. J., Huang, Y., Kleinjung, J., Wilson, V. and
487 Briscoe, J.** (2014). In vitro generation of neuromesodermal progenitors reveals distinct
488 roles for wnt signalling in the specification of spinal cord and paraxial mesoderm
489 identity. *PLoS Biol.* **12**, e1001937.
- 490 **Graf, T. and Enver, T.** (2009). Forcing cells to change lineages. *Nature* **462**, 587–594.
- 491 **Haupaix, N., Abitua, P. B., Sirour, C., Yasuo, H., Levine, M. and Hudson, C.** (2014).
492 Ephrin-mediated restriction of ERK1/2 activity delimits the number of pigment cells in
493 the *Ciona* CNS. *Dev. Biol.* **394**, 170–180.
- 494 **Henrique, D., Abranches, E., Verrier, L. and Storey, K. G.** (2015). Neuromesodermal
495 progenitors and the making of the spinal cord. *Development* **142**, 2864–2875.
- 496 **Henry, J. Q., Perry, K. J., Wever, J., Seaver, E. and Martindale, M. Q.** (2008). Beta-
497 catenin is required for the establishment of vegetal embryonic fates in the nemertean,
498 *Cerebratulus lacteus*. *Dev. Biol.* **317**, 368–379.
- 499 **Hudson, C. and Yasuo, H.** (2008). Similarity and diversity in mechanisms of muscle fate
500 induction between ascidian species. *Biol. Cell* **100**, 265–277.
- 501 **Hudson, C., Darras, S., Caillol, D., Yasuo, H. and Lemaire, P.** (2003). A conserved role
502 for the MEK signalling pathway in neural tissue specification and posteriorisation in the
503 invertebrate chordate, the ascidian *Ciona intestinalis*. *Development* **130**, 147–159.
- 504 **Hudson, C., Kawai, N., Negishi, T. and Yasuo, H.** (2013). β -Catenin-Driven Binary Fate

- 505 Specification Segregates Germ Layers in Ascidian Embryos. *Curr. Biol.* **23**, 491–495.
- 506 **Hudson, C.** (2016). The central nervous system of ascidian larvae. *Wiley*
507 *Interdisciplinary Reviews. Developmental Biology* doi: **10.1002/wdev.239**.
- 508 **Imai, K. S.** (2003). Isolation and characterization of beta-catenin downstream genes in
509 early embryos of the ascidian *Ciona savignyi*. *Differentiation* **71**, 346–360.
- 510 **Imai, K., Takada, N., Satoh, N. and Satou, Y.** (2000). (beta)-catenin mediates the
511 specification of endoderm cells in ascidian embryos. *Development* **127**, 3009–3020.
- 512 **Imai, K. S., Satoh, N. and Satou, Y.** (2002a). Early embryonic expression of FGF4/6/9
513 gene and its role in the induction of mesenchyme and notochord in *Ciona savignyi*
514 embryos. *Development* **129**, 1729–1738.
- 515 **Imai, K. S., Satou, Y. and Satoh, N.** (2002b). Multiple functions of a Zic-like gene in the
516 differentiation of notochord, central nervous system and muscle in *Ciona savignyi*
517 embryos. *Development* **129**, 2723–2732.
- 518 **Imai, K. S., Satoh, N. and Satou, Y.** (2002c). An essential role of a FoxD gene in
519 notochord induction in *Ciona* embryos. *Development* **129**, 3441–3453.
- 520 **Imai, K. S., Hino, K., Yagi, K., Satoh, N. and Satou, Y.** (2004). Gene expression profiles
521 of transcription factors and signaling molecules in the ascidian embryo: towards a
522 comprehensive understanding of gene networks. *Development* **131**, 4047–4058.
- 523 **Imai, K. S., Levine, M., Satoh, N. and Satou, Y.** (2006). Regulatory blueprint for a
524 chordate embryo. *Science* **312**, 1183–1187.
- 525 **Kiecker, C., Bates, T. and Bell, E.** (2016). Molecular specification of germ layers in
526 vertebrate embryos. *Cell. Mol. Life Sci.* **73**, 923–947.
- 527 **Kim, G. J. and Nishida, H.** (2001). Role of the FGF and MEK signaling pathway in the
528 ascidian embryo. *Dev. Growth Differ.* **43**, 521–533.
- 529 **Kimelman, D. and Griffin, K. J.** (2000). Vertebrate mesendoderm induction and
530 patterning. *Curr. Opin. Genet. Dev.* **10**, 350–356.
- 531 **Kubo, A., Suzuki, N., Yuan, X., Nakai, K., Satoh, N., Imai, K. S. and Satou, Y.** (2010).
532 Genomic cis-regulatory networks in the early *Ciona intestinalis* embryo. *Development*
533 **137**, 1613–1623.
- 534 **Kumano, G., Yamaguchi, S. and Nishida, H.** (2006). Overlapping expression of FoxA
535 and Zic confers responsiveness to FGF signaling to specify notochord in ascidian
536 embryos. *Developmental Biology* **300**, 770–784.
- 537 **Lamy, C., Rothbächer, U., Caillol, D. and Lemaire, P.** (2006). Ci-FoxA-a is the earliest
538 zygotic determinant of the ascidian anterior ectoderm and directly activates Ci-sFRP1/5.
539 *Development* **133**, 2835–2844.
- 540 **Logan, C. Y., Miller, J. R., Ferkowicz, M. J. and McClay, D. R.** (1999). Nuclear beta-
541 catenin is required to specify vegetal cell fates in the sea urchin embryo. *Development*
542 **126**, 345–357.

- 543 **Maduro, M. F., Meneghini, M. D., Bowerman, B., Broitman-Maduro, G. and Rothman,**
544 **J. H.** (2001). Restriction of mesendoderm to a single blastomere by the combined action
545 of SKN-1 and a GSK-3beta homolog is mediated by MED-1 and -2 in *C. elegans*. *Mol. Cell*
546 **7**, 475–485.
- 547 **Maduro, M. F., Broitman-Maduro, G., Choi, H., Carranza, F., Wu, A. C.-Y. and Rifkin, S.**
548 **A.** (2015). MED GATA factors promote robust development of the *C. elegans* endoderm.
549 *Dev. Biol.* **404**, 66–79.
- 550 **Martin, B. L. and Kimelman, D.** (2012). Canonical Wnt signaling dynamically controls
551 multiple stem cell fate decisions during vertebrate body formation. *Dev. Cell* **22**, 223–
552 232.
- 553 **McCauley, B. S., Akyar, E., Saad, H. R. and Hinman, V. F.** (2015). Dose-dependent
554 nuclear β -catenin response segregates endomesoderm along the sea star primary axis.
555 *Development* **142**, 207–217.
- 556 **McGhee, J. D.** (2013). The *Caenorhabditis elegans* intestine. *Wiley Interdiscip Rev Dev*
557 *Biol* **2**, 347–367.
- 558 **Meijer, L., Skaltsounis, A.-L., Magiatis, P., Polychronopoulos, P., Knockaert, M.,**
559 **Leost, M., Ryan, X. P., Vonica, C. A., Brivanlou, A., Dajani, R., et al.** (2003). GSK-3-
560 selective inhibitors derived from Tyrian purple indirubins. *Chem. Biol.* **10**, 1255–1266.
- 561 **Minokawa, T., Yagi, K., Makabe, K. W. and Nishida, H.** (2001). Binary specification of
562 nerve cord and notochord cell fates in ascidian embryos. *Development* **128**, 2007–2017.
- 563 **Miya, T. and Nishida, H.** (2003). An Ets transcription factor, HrEts, is target of FGF
564 signaling and involved in induction of notochord, mesenchyme, and brain in ascidian
565 embryos. *Dev. Biol.* **261**, 25–38.
- 566 **Miyawaki, K., Yamamoto, M., Saito, K., Saito, S., Kobayashi, N. and Matsuda, S.**
567 (2003). Nuclear localization of beta-catenin in vegetal pole cells during early
568 embryogenesis of the starfish *Asterina pectinifera*. *Dev. Growth Differ.* **45**, 121–128.
- 569 **Momose, T. and Houliston, E.** (2007). Two oppositely localised frizzled RNAs as axis
570 determinants in a cnidarian embryo. *PLoS Biol.* **5**, e70.
- 571 **Nicol, D. and Meinertzhagen, I. A.** (1988). Development of the central nervous system
572 of the larva of the ascidian, *Ciona intestinalis* L. I. The early lineages of the neural plate.
573 *Dev. Biol.* **130**, 721–736.
- 574 **Nimmo, R. A., May, G. E. and Enver, T.** (2015). Primed and ready: understanding
575 lineage commitment through single cell analysis. *Trends Cell Biol.* **25**, 459–467.
- 576 **Nishida, H.** (1987). Cell lineage analysis in ascidian embryos by intracellular injection of
577 a tracer enzyme. III. Up to the tissue restricted stage. *Dev. Biol.* **121**, 526–541.
- 578 **Nishida, H.** (2003). Spatio-temporal pattern of MAP kinase activation in embryos of the
579 ascidian *Halocynthia roretzi*. *Dev. Growth Differ.* **45**, 27–37.
- 580 **Oda-Ishii, I., Kubo, A., Kari, W., Suzuki, N., Rothbächer, U. and Satou, Y.** (2016). A
581 Maternal System Initiating the Zygotic Developmental Program through Combinatorial

- 582 Repression in the Ascidian Embryo. *PLoS Genet.* **12**, e1006045.
- 583 **Ohta, N. and Satou, Y.** (2013). Multiple signaling pathways coordinate to induce a
584 threshold response in a chordate embryo. *PLoS Genet.* **9**, e1003818.
- 585 **Pasini, A., Manenti, R., Rothbächer, U. and Lemaire, P.** (2012). Antagonizing Retinoic
586 Acid and FGF/MAPK Pathways Control Posterior Body Patterning in the Invertebrate
587 Chordate *Ciona intestinalis*. *PLoS One* **7**.
- 588 **Peter, I. S. and Davidson, E. H.** (2010). The endoderm gene regulatory network in sea
589 urchin embryos up to mid-blastula stage. *Dev. Biol.* **340**, 188–199.
- 590 **Picco, V., Hudson, C. and Yasuo, H.** (2007). Ephrin-Eph signalling drives the
591 asymmetric division of notochord/neural precursors in *Ciona* embryos. *Development*
592 **134**, 1491–1497.
- 593 **Rodaway, A. and Patient, R.** (2001). Mesendoderm. an ancient germ layer? *Cell* **105**,
594 169–172.
- 595 **Rothbächer, U., Bertrand, V., Lamy, C. and Lemaire, P.** (2007). A combinatorial code
596 of maternal GATA, Ets and beta-catenin-TCF transcription factors specifies and patterns
597 the early ascidian ectoderm. *Development* **134**, 4023–4032.
- 598 **Roure, A., Rothbächer, U., Robin, F., Kalmar, E., Ferone, G., Lamy, C., Missero, C.,
599 Mueller, F. and Lemaire, P.** (2007). A multicassette Gateway vector set for high
600 throughput and comparative analyses in *ciona* and vertebrate embryos. *PLoS ONE* **2**,
601 e916.
- 602 **Row, R. H., Tsotras, S. R., Goto, H. and Martin, B. L.** (2016). The zebrafish tailbud
603 contains two independent populations of midline progenitor cells that maintain long-
604 term germ layer plasticity and differentiate in response to local signaling cues.
605 *Development* **143**, 244–254.
- 606 **Sardet, C., McDougall, A., Yasuo, H., Chenevert, J., Pruliere, G., Dumollard, R.,
607 Hudson, C., Hebras, C., Le Nguyen, N. and Paix, A.** (2011). Embryological methods in
608 ascidians: the Villefranche-sur-Mer protocols. *Methods Mol. Biol.* **770**, 365–400.
- 609 **Satou, Y., Imai, K. S. and Satoh, N.** (2001). Early embryonic expression of a LIM-
610 homeobox gene Cs-lhx3 is downstream of beta-catenin and responsible for the
611 endoderm differentiation in *Ciona savignyi* embryos. *Development* **128**, 3559–3570.
- 612 **Satou, Y., Yamada, L., Mochizuki, Y., Takatori, N., Kawashima, T., Sasaki, A.,
613 Hamaguchi, M., Awazu, S., Yagi, K., Sasakura, Y., et al.** (2002). A cDNA resource from
614 the basal chordate *Ciona intestinalis*. *Genesis* **33**, 153–154.
- 615 **Shi, W. and Levine, M.** (2008). Ephrin signaling establishes asymmetric cell fates in an
616 endomesoderm lineage of the *Ciona* embryo. *Development* **135**, 931–940.
- 617 **Shirae-Kurabayashi, M., Matsuda, K. and Nakamura, A.** (2011). Ci-Pem-1 localizes to
618 the nucleus and represses somatic gene transcription in the germline of *Ciona*
619 intestinalis embryos. *Development* **138**, 2871–2881.
- 620 **Stolfi, A., Sasakura, Y., Chalopin, D., Satou, Y., Christiaen, L., Dantec, C., Endo, T.,**

- 621 **Naville, M., Nishida, H., Swalla, B. J., et al.** (2015). Guidelines for the nomenclature of
622 genetic elements in tunicate genomes. *Genesis* **53**, 1–14.
- 623 **Sulston, J. E. and Horvitz, H. R.** (1977). Post-embryonic cell lineages of the nematode,
624 *Caenorhabditis elegans*. *Dev. Biol.* **56**, 110–156.
- 625 **Sulston, J. E., Schierenberg, E., White, J. G. and Thomson, J. N.** (1983). The embryonic
626 cell lineage of the nematode *Caenorhabditis elegans*. *Dev. Biol.* **100**, 64–119.
- 627 **Tremblay, K. D.** (2010). Formation of the murine endoderm: lessons from the mouse,
628 frog, fish, and chick. *Prog Mol Biol Transl Sci* **96**, 1–34.
- 629 **Tzouanacou, E., Wegener, A., Wymeersch, F. J., Wilson, V. and Nicolas, J.-F.** (2009).
630 Redefining the progression of lineage segregations during mammalian embryogenesis
631 by clonal analysis. *Dev. Cell* **17**, 365–376.
- 632 **Valenta, T., Hausmann, G. and Basler, K.** (2012). The many faces and functions of β -
633 catenin. *EMBO J.* **31**, 2714–2736.
- 634 **Whittaker, J. R.** (1977). Segregation during cleavage of a factor determining
635 endodermal alkaline phosphatase development in ascidian embryos. *J. Exp. Zool.* **202**,
636 139–153.
- 637 **Wikramanayake, A. H., Huang, L. and Klein, W. H.** (1998). beta-Catenin is essential for
638 patterning the maternally specified animal-vegetal axis in the sea urchin embryo. *Proc.
639 Natl. Acad. Sci. U.S.A.* **95**, 9343–9348.
- 640 **Wikramanayake, A. H., Hong, M., Lee, P. N., Pang, K., Byrum, C. A., Bince, J. M., Xu, R.
641 and Martindale, M. Q.** (2003). An ancient role for nuclear beta-catenin in the evolution
642 of axial polarity and germ layer segregation. *Nature* **426**, 446–450.
- 643 **Yasuo, H. and Hudson, C.** (2007). FGF8/17/18 functions together with FGF9/16/20
644 during formation of the notochord in *Ciona* embryos. *Dev. Biol.* **302**, 92–103.
- 645
- 646

648 **Figure 1. Foxa.a, Foxd and Fgf9/16/20 are candidate NNE lineage specification factors.**
 649 a) Schematic drawings of embryos at the 16- and 32-cell stage. In this and all subsequent
 650 figures, where shown, a green dashed line separates the animal (ectoderm) from the vegetal
 651 (mesendoderm) hemispheres and a brown dashed line separates A- (A4.1) and a- (a4.2)
 652 lineages from B- (B4.1) and b- (b4.2) lineages. Different embryonic founder lineages are
 653 indicated on the drawings. NN and E cells are indicated in red and blue respectively. Below
 654 the embryo drawing is a schematic representation of the two rounds of n β -catenin-driven
 655 binary fate decisions that segregate firstly the mesendoderm lineages from the ectoderm
 656 lineages at the 16-cell stage and secondly segregate the mesoderm (NN) lineages from the
 657 endoderm (E) lineages at the 32-cell stage (Hudson et al., 2013). b, c) Embryos analysed at
 658 the 16-cell stage for the marker indicated to the left of the panels following the treatment
 659 indicated above the panels. The numbers on the bottom-left corner of each panel indicates the
 660 proportion of embryos that the panel represents. The posterior most cells (at the bottom of the
 661 panels) are transcriptionally quiescent cells that will generate the germ line (Shirae-
 662 Kurabayashi et al., 2011). For *Foxa.a* expression in (b) control embryos showed expression in
 663 all four A-line (NNE) cells in 34/34 embryos, and in B-line cells, in 15/34 embryos, as
 664 indicated, whereas β -catenin-MO (β -cat-MO) injected embryos showed expression in NNE
 665 cells (31/31), but not B-line (0/31). Expression of *Foxa.a* in the four a-line precursors (not
 666 visible in the image) was not affected by β -catenin-MO injection.

667

668 **Figure 2. Foxa.a, Foxd and Fgf9/16/20 are required for initiation of NN and E gene
 669 expression.** a) Embryos analysed at the 32-cell stage. The marker analysed is indicated on the
 670 left of the panels and the treatment indicated above the panels. The average number of NN
 671 (Zic-r.b) or E (Lhx3/4) cells expressing detectable levels of each gene is indicated. This
 672 remaining expression was generally weaker than control level expression. ‘n=’ represents the
 673 number of embryos analysed. b) Expression of *Efna.d* under the conditions indicated. The
 674 graph shows the average number of cells expressing *Efna.d* in different vegetal lineages at the
 675 32-cell stage, as indicated by the key. All embryos showed ectoderm expression. The number
 676 of embryos analysed is indicated above the bars on the graph.

677 The following supplements are available for figure 2.

678 **Figure 2-figure supplement 1.** *Foxa.a, Foxd and Fgf9/16/20 are required for initiation of*
 679 *NN and E gene expression.*

680 **Figure 2-figure supplement 2.** Endoderm formation under various conditions.

681

682 **Figure 3. Creation of an ectopic Foxa.a, Foxd, Fgf-signal overlap leads to ectopic**
 683 **mesendoderm formation.** a) Schematics show endogenous ectodermal expression of *Foxa.a*,
 684 *Foxd* (no expression) and activation of ERK (dpERK), indicated by blue dots. b-c) Treatment
 685 is indicated above the panels and marker analysed to the left. Numbers show the total average
 686 number of cells per embryo expressing each marker. n= total number of embryos analysed.
 687 The graphs show the average number of cells expressing each maker in the lineages indicated

688 on the keys, following the treatments indicated of the x-axis. No *Zic-r.b* expression was
689 detected in endoderm lineages. In (c) the green arrowheads highlight the eight a-lineage cells.
690 For (b), representative panels of uninjected/UO-treated and uninjected/BIO-treated embryos
691 are not shown. The numbers of these experiments are: for *Zic-r.b*- U0126 alone n=40 (average
692 number of cells 2.6), BIO-16 alone n= 40 (average number of cells 2.9) and for *Bra*- U0126
693 alone, n=39 (average number of cells 0.0); BIO-16 alone n=31 (average number of cells 0.0).

694 The following supplements are available for figure 3.

695 **Figure 3-figure supplement 1.** *Foxd* mRNA injection leads to repression of *Efna.d* and
696 upregulation of *Fgf9/16/20* in ectodermal cells at the 16-cell stage.

697

698 **Figure 4. *Foxd* mRNA injection rescues mesoderm in β -catenin-MO injected embryos.** a-
699 b) Treatment is indicated above the panels and marker analysed to the left of the panels. The
700 total average number of cells per embryo is indicated, ‘n’ indicates the total number of
701 embryos analysed for each treatment. The graphs show the average number of cells
702 expressing each marker in the lineages indicated by the keys, following the treatments
703 indicated.

704

705 **Figure 5. Reprogramming the ectoderm lineage to mesendoderm.** a) Experimental
706 scheme. Embryos were electroporated and the ectoderm lineage (animal cap) isolated at the 8-
707 cell stage. Ectodermal explants were cultured until the mid-gastrula stage for *Lhx3/4*
708 expression or at the neurula stage for *Bra* expression. Optionally, explants were treated with
709 BIO, when control sibling embryos reached the 76-cell stage, for approximately one hour
710 prior to fixation (*Lhx3/4* only). b-c) Expression of *Bra* (b) and *Lhx3/4* (c) in isolated
711 ectodermal explants, following the treatments indicated above the panels. ‘n’ represents the
712 number of explants analysed. Graphs shows the percentage of explants with any level of *Bra*
713 expression or level of *Lhx3/4* expression indicated by the key, under various conditions
714 (Foxa.a=pFT>Foxa.a; Foxd = pFT>Foxy; Fgf9= pFT>Fgf9/16/20; control =
715 unelectroporated).

716 The following supplements are available for figure 5.

717 **Figure 5-figure supplement 1.** Reprogramming of ectoderm cells to mesendoderm fates.

718 **Figure 5-figure supplement 2.** Confirmation that BIO-treatment of ectoderm explants at
719 the 76-cell stage results in nuclear localisation of β -catenin.

720

721 **Figure 6. Gene regulatory model for segregation of NNE into NN and E lineages.**

722 a) Each factor induced by n β -catenin activation at the 16-cell stage feeds into both the NN
723 and E lineage genes. The dashed line for *Fgf9/16/20* represents a signalling molecule (most
724 likely mediated, at least in part, by Ets1/2 transcription factor (Table 1). Differential gene
725 expression between NN and E cells is mediated by the second n β -catenin-driven switch. b-c)
726 Schematic regulatory architectures during mesendoderm segregation. ME= mesendoderm
727 lineage; M= mesoderm lineage; E= endoderm lineage; e= endoderm gene; m= mesoderm

728 gene; X, Y = genes expressed in mesendoderm cells. b) Ascidian and nematode mesendoderm
729 regulatory architecture. (b) ‘Mixed-lineage’ mesendoderm regulatory architecture.

730

731

	Control	U0126	ETS1/2-MO
Zic-r.b NN cell	4.0 cells (n=163)	0.75 cells (n=58)	3.4 cells* (n=74)
Lhx3/4 E cell	3.9 cells (n=153)	2.1** cell (n=45)	0.7 cells (n=92)

732

733 **Table 1.** Expression of *Zic-r.b* in NN cells and *Lhx3/4* in E cells of 32-cell stage embryos,
 734 following inhibition of Fgf-signalling components. * 44/74 embryos exhibited weaker
 735 levels of *Zic-r.b* expression compared to controls ** remaining expression was weaker
 736 than control levels of expression.

737

738 **SUPPLEMENTARY**

739 **Figure 2-figure supplement 1. Foxa.a, Foxd and Fgf9/16/20 are required for**
740 **initiation of NN and E gene expression.** a-b) Embryos analysed at the 32-cell, 64-cell,
741 or early gastrula stage (eG), as indicated, for the marker indicated to the left of the
742 panels and following the treatment indicated above the panels. For the top three rows of
743 panels, the proportion of embryos that the panel represents is shown. For *Foxd*
744 expression, embryos were counted if at least 5 E cells show expression, regardless of
745 level; for *Fgf9/16/20* and *Foxa.a*, embryos were scored positive if at least 3 NN and 3 A-
746 line E cells showed expression, regardless of level. Expression in other domains of the
747 embryo were also not affected by these treatments, except for *Foxd* expression in NN
748 cells which appeared slightly increased in U0126 treated embryos (control embryos
749 displayed an average of 0.2 cells strong and 0.6 cells weak expression in NN cells,
750 U0126-treated embryos displayed an average of 0.9 cells strong and 0.9 cells weak
751 expression). 64-cell stage expression of *Zic-r.b* is presented as the average number of NN
752 lineage cells with expression. The result for *Fgf9-MO* is included in the U0126 panel.
753 *Lhx3/4* is presented as the average number of cells expressing per embryo. For *Titf*, the
754 numbers indicate the proportion of embryos that the panel represents. c-e) The
755 percentage of embryo halves showing detectable (strong and weak) *Lhx3/4* expression
756 in each lineage following the treatments indicated. n= the number of embryos halves
757 scored. A 50% reduction in expression compared to controls is indicated in red. Note the
758 preferential loss of marginal (notochord and mesenchyme lineage) expression
759 compared to endoderm lineage expression following Fox gene inhibition. f) ERK1/2
760 activation at the 32-cell stage depends on *Fgf9/16/20*. Anti-dpERK immunofluorescence
761 was carried out on mid-32 cell stage embryos for vegetal dpERK detection and late 32-
762 cell stage embryos for the animal cells. The average number of NN, E and animal cells
763 per embryo exhibiting dpERK activity are shown. NN cells generally exhibited weaker
764 ERK activity compared to E cells. 'n=' indicates the total number of embryos analysed.

765

766 **Figure 2-figure supplement 2. Endoderm formation under various conditions.**
767 Detection of alkaline phosphatase activity under the conditions indicated above the
768 panels. Fgf9=Fgf9/16/20; Fgf8=Fgf8/17/18. Endoderm is lost with *Foxa.a-MO* or a
769 combination of *Foxd-MO/U0126*. Small amounts of endoderm remain in *Foxd-MO/Fgf9-*
770 *MO* embryos. We have previously shown that *Fgf8/17/18*, expressed from the 64-cell
771 stage, cooperates with *Fgf9/16/20* during notochord induction(Yasuo and Hudson,
772 2007). Co-inhibition of *Fgf9/16/20*, *Fgf8/17/18* and *Foxd* led to a stronger down
773 regulation of alkaline phosphatase, suggesting that *Fgf8/17/18* cooperates with
774 *Fgf9/16/20* during endoderm induction. The graphs shows the proportion of embryos
775 (%) with strong and reduced (compared to control) alkaline phosphatase activity, as
776 indicated on the key, following the treatments indicated on the left. 'n=' indicates the
777 number of embryos analysed.

778

779 **Figure 3-figure supplement 1. *Foxd* mRNA injection leads to repression of *Efna.d***
780 **and upregulation of *Fgf9/16/20* in ectodermal cells at the 16-cell stage.** Treatment

781 is indicated above the panels and gene expression analysed to the left of the panels. The
782 arrowheads indicate weak ectopic expression. Numbers indicated the proportion of
783 embryos that the panel represents. *Foxa.a* expression is not effected.

784

785 **Figure 4-figure supplement 1. Reprogramming of ectoderm cells to mesendoderm**
786 **fates.** 32c=32-cell stage; 64c=64-cell stage; 76c=76-cell stage; 110c=110-cell stage; eG=
787 early gastrula stage (approximately 3-row neural plate stage); 6R=6-row neural plate
788 stage (mid-gastrula); neur=neurula stage. a) Determining the onset of promoter activity
789 of the *Fucosyltransferase-like* gene. The pFT>*Foxd* construct was electroporated and
790 embryos were fixed at different developmental time points and assayed for *Foxd*
791 expression in ectoderm cells by *in situ* hybridisation. The graph shows the percentage of
792 embryos showing any level of *Foxd* expression in ectoderm cells in four independent
793 experiments. The number of embryos counted per bar on the graph is indicated above
794 the bar. nd= not done. On the right are shown examples of *Foxd* *in situ* hybridisations on
795 electroporated embryos at the time points indicated. b-c) FT>x3= pFT>*Foxa.a* +
796 pFT>*Foxd* + pFT>*Fgf9/16/20*; FT>Tom= pFT>tdTomato (as a control electroporation);
797 Cont. = unelectroporated embryos. b) The ectoderm genetic programme is down-
798 regulated in FT>x3 electroporated embryos. Electroporated embryos were analysed for
799 *Efna.d* at the 32-cell stage, *DllB* at the 64-cell to 6-row neural plate stage, and *Epi-1* at the
800 neurula stage. The graph shows the percentage of embryos with ectoderm gene
801 expression corresponding to 50% or more of control levels (estimated based on size of
802 expression domain), under the conditions indicated by the key. nd= not done. c) *Zic-r.b* is
803 ectopically activated in non-neural ectoderm cells in FT>x3 electroporated embryos.
804 The graph shows the percentage of embryos with any level of ectopic *Zic-r.b* expression
805 in ectoderm cells, under the conditions indicated by the key. nd= not done.

806

807 **Figure 5-figure supplement 1. Confirmation that BIO-treatment of ectoderm**
808 **explants at the 76-cell stage results in nuclear localisation of β-catenin.** Explants
809 were treated with BIO for 30 minutes and then immunostained with β-catenin
810 antibodies and counterstained with DAPI. Panels show single z-slices of confocal images.
811 Numbers indicate the number of interphase cells with nuclear β-catenin. A total of 11
812 ectoderm explants were counted for control and 15 for BIO-treated.

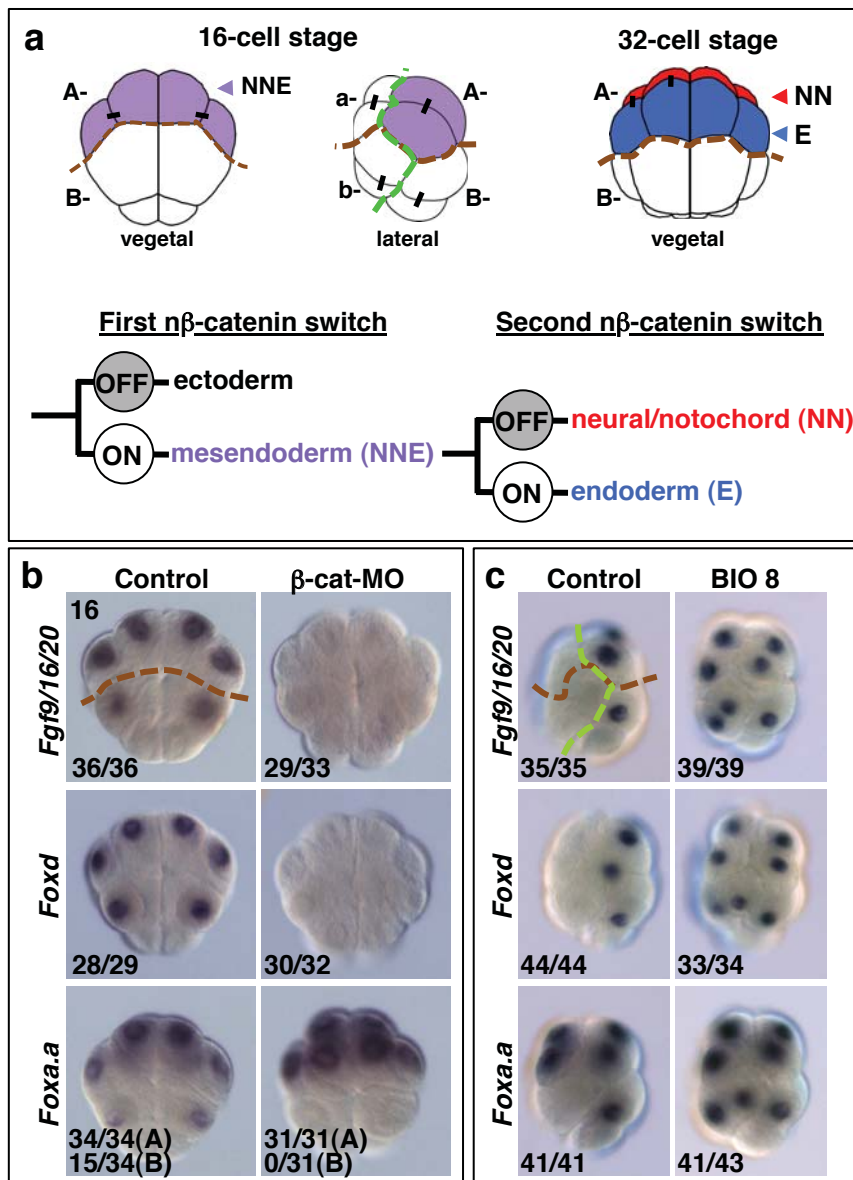


Figure 1 (Hudson)

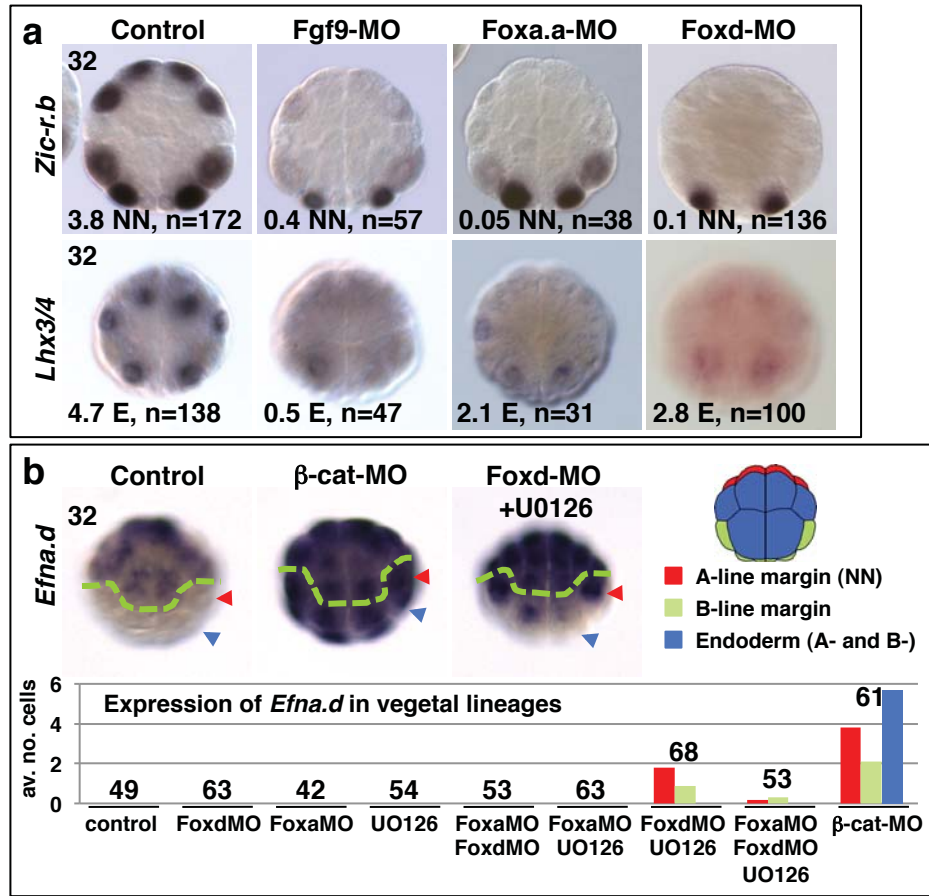


Figure 2 (Hudson)

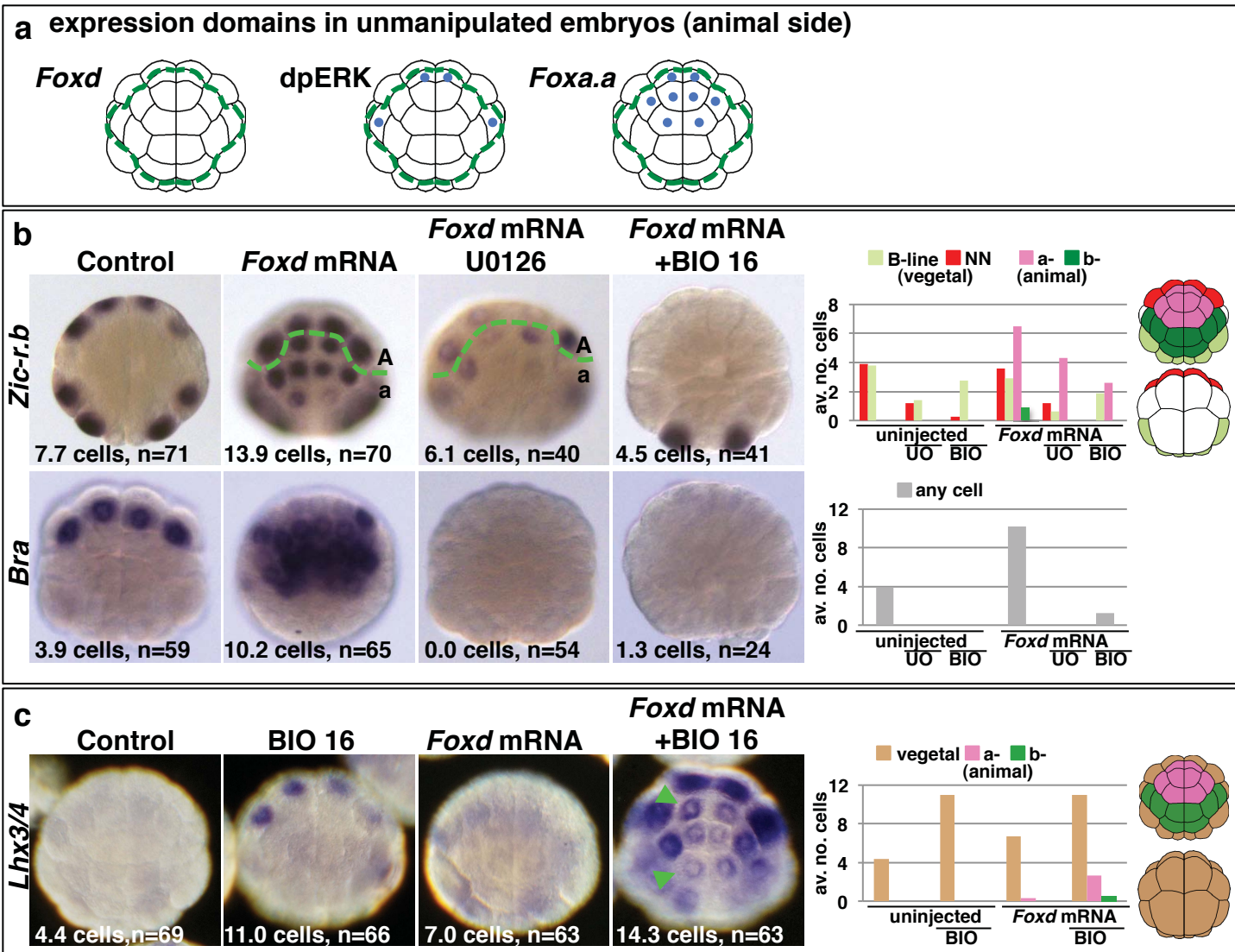


Figure 3 (Hudson)

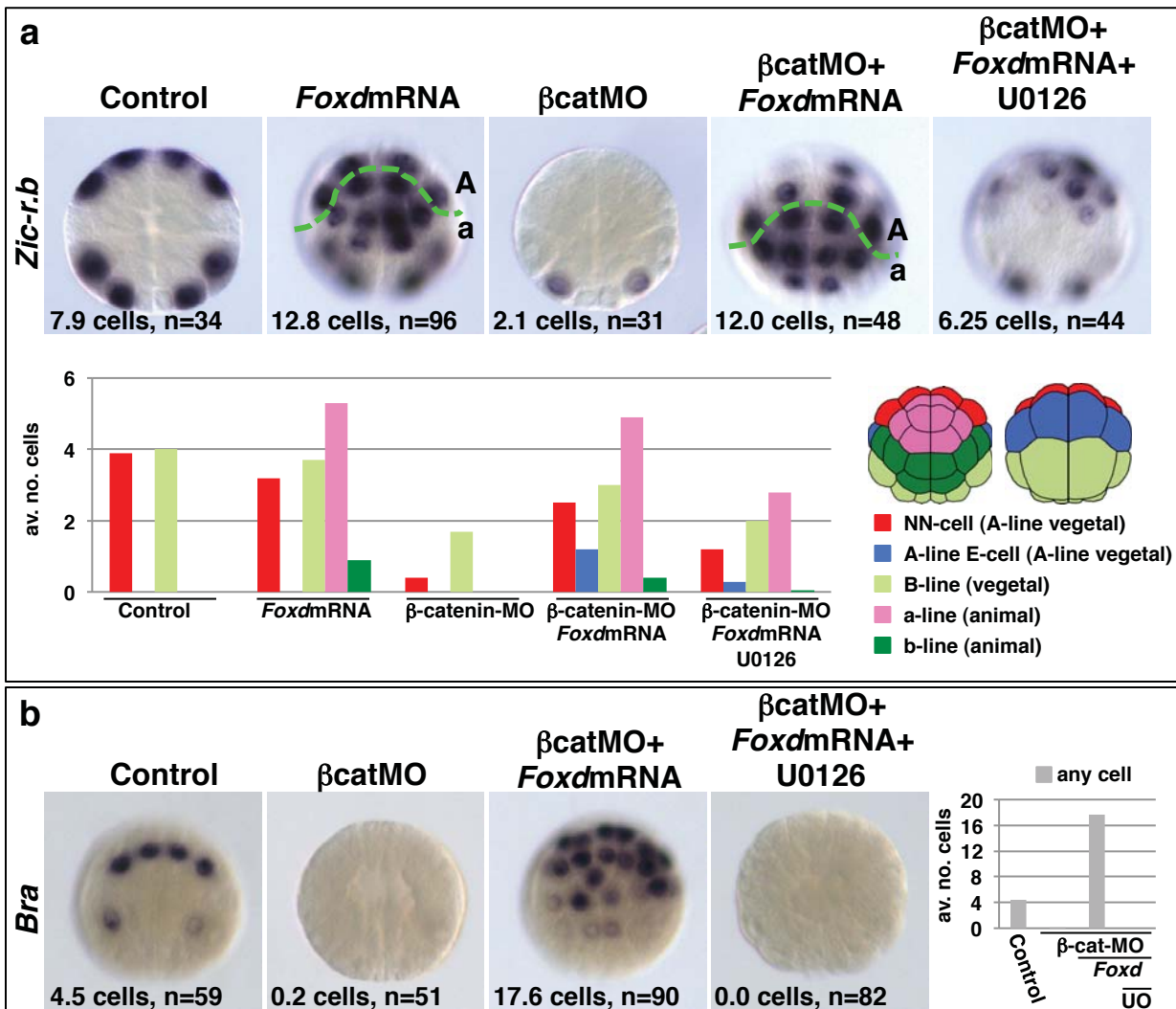


Figure 4 (Hudson)

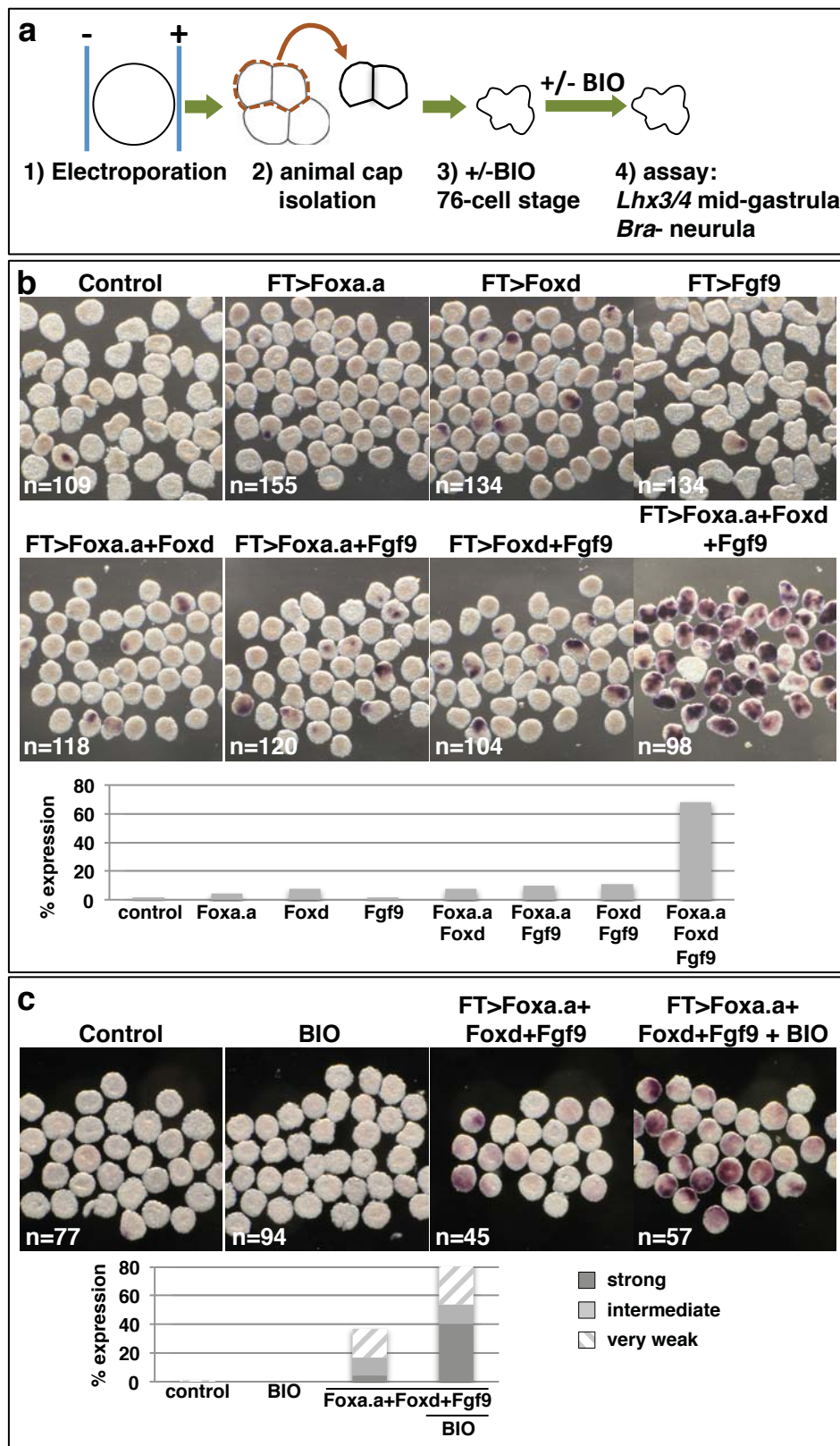


Figure 5 (Hudson)

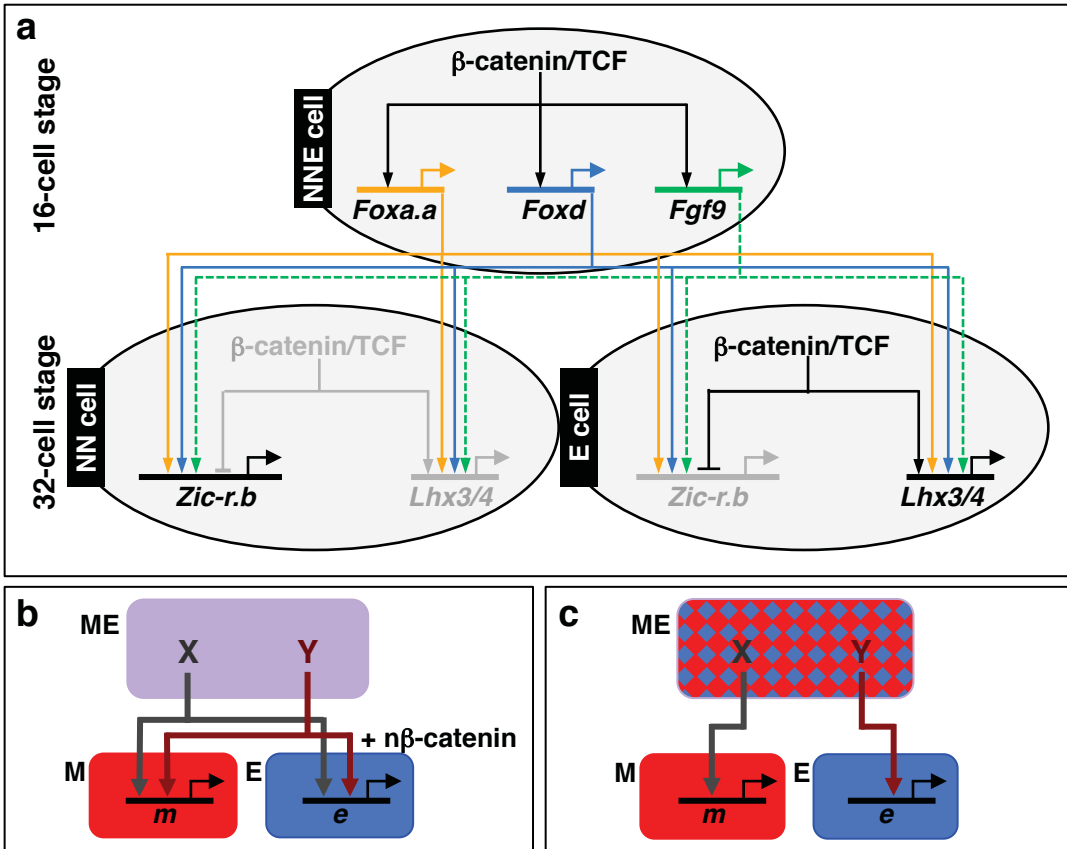


Figure 6 (Hudson)